Acta Pharmaceutica Sinica B 2019;9(4):724–733

Chinese Pharmaceutical Association
Institute of Materia Medica, Chinese Academy of Medical Sciences

Acta Pharmaceutica Sinica B

www.elsevier.com/locate/apsb
www.sciencedirect.com

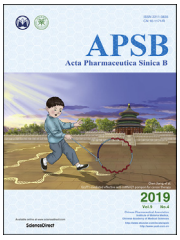

ORIGINAL ARTICLE

Emodin alleviates cardiac fibrosis by suppressing activation of cardiac fibroblasts *via* upregulating metastasis associated protein 3

Dan Xiao[a,†], Yue Zhang[a,†], Rui Wang[a,†], Yujie Fu[a], Tong Zhou[b], Hongtao Diao[a], Zhixia Wang[a], Yuan Lin[a], Zhange Li[a], Lin Wen[a], Xujuan Kang[a], Philipp Kopylov[c], Dmitri Shchekochikhin[c], Yong Zhang[a,d,*], Baofeng Yang[a,e,*]

[a]*Department of Pharmacology (State-Province Key Laboratories of Biomedicine-Pharmaceutics of China, Key Laboratory of Cardiovascular Research, Ministry of Education), Harbin Medical University, Harbin 150081, China*
[b]*Department of Pharmacy, The First Affiliated Hospital of Harbin Medical University, Harbin 150081, China*
[c]*Department of Preventive and Emergency Cardiology, Sechenov First Moscow State Medical University, Moscow 119991, Russian Federation*
[d]*Institute of Metabolic Disease, Heilongjiang Academy of Medical Science, Harbin 150086, China*
[e]*Department of Pharmacology and Therapeutics, Melbourne School of Biomedical Sciences, Faculty of Medicine, Dentistry and Health Sciences, The University of Melbourne, Melbourne 3010, Australia*

Received 13 November 2018; received in revised form 21 March 2019; accepted 2 April 2019

KEY WORDS

Emodin;
Cardiac fibrosis;
MTA3;
Angiotensin II;
Cardiac fibroblast;
Mouse

Abstract Excess activation of cardiac fibroblasts inevitably induces cardiac fibrosis. Emodin has been used as a natural medicine against several chronic diseases. The objective of this study is to determine the effects of emodin on cardiac fibrosis and the underlying molecular mechanisms. Intragastric administration of emodin markedly decreased left ventricular wall thickness in a mouse model of pathological cardiac hypertrophy with excess fibrosis induced by transaortic constriction (TAC) and suppressed activation of cardiac fibroblasts induced by angiotensin II (AngII). Emodin upregulated expression of metastasis associated protein 3 (MTA3) and restored the MTA3 expression in the setting of cardiac fibrosis. Moreover, overexpression of MTA3 promoted cardiac fibrosis; in contrast, silence of MTA3 abrogated the inhibitory effect of emodin on fibroblast activation. Our findings unraveled the potential of emodin to alleviate cardiac fibrosis *via* upregulating MTA3 and highlight the regulatory role of MTA3 in the development of cardiac fibrosis.

*Corresponding authors. Tel.: +86 451 86671354; fax: +86 451 86669482.
E-mail addresses: hmuzhangyong@hotmail.com (Yong Zhang), yangbf@ems.hrbmu.edu.cn (Baofeng Yang).
[†]These authors made equal contributors to this work.
Peer review under responsibility of Institute of Materia Medica, Chinese Academy of Medical Sciences and Chinese Pharmaceutical Association.

https://doi.org/10.1016/j.apsb.2019.04.003

1. Introduction

Cardiac fibrosis refers to excess activation of cardiac fibroblasts and the consequent accumulation of abnormal extracellular matrix (ECM)[1]. In response to prolonged stress, development of cardiac fibrosis contributes to a stiffer and less compliant heart[2]. Cardiac fibrosis is characterized as an intricate progression contributing to adverse cardiac structural remodeling[3], which may eventually lead to heart failure.

In the development of cardiac fibrosis, numerous studies have reported therapeutic potential of emodin, a natural anthraquinone derivative found in many traditional Chinese medicines (TCM), on various chronic diseases[4]. For example, emodin can produce protective effects on atherosclerosis[5], myocarditis[6], cardiovascular homeostasis[7], and Goldblatt hypertension-induced cardiac fibrosis[8]. Since its introduction to the field in 1920s, emodin has attracted tremendous interest because of its high safety profiles and multiple pharmacological functions[9]. Of note, the antifibrotic role of emodin has been recently addressed. In the setting of lung fibrosis, emodin improves pulmonary function by targeting SIRT1 signaling[10]. Emodin ameliorates the peritoneal dialysis-related peritoneal fibrosis *via* inhibiting the Notch pathway[11]. Clearly, emodin possesses anti-fibrotic property in many organs/tissues; however, whether it also has an effect on cardiac fibrosis remained unknown.

Studies have demonstrated that metastasis-associated protein 3 (MTA3) regulates various cellular events[12], and acts primarily as a tumor suppressor[13]. It influences E-cadherin expression in breast cancer cells by inhibiting epithelial-to-mesenchymal transition (EMT)[14]. Cardiac fibroblasts are generated during EMT progression, suggesting the potential of MTA3 in regulating cardiac fibroblasts[15]. Additionally, MTA3 is well-documented as an inhibitor against cell proliferation and migration[16]. Previous studies have unraveled that MTA3 expression correlates with cardiac fibrosis[17,18]. Thus, we hypothesized that MTA3 may play an essential role in suppressing the proliferation and migration of cardiac fibroblasts.

The objectives of this study were to investigate the beneficial effects of emodin on cardiac fibrosis and the involvement of MTA3 as mediator of emodin action in this process. To this end, we conducted a series of experiments with both *in vivo* and *in vitro* cardiac fibrotic models and identified emodin as an anti-fibrotic agent acting by upregulating MTA3 as a molecular mechanism.

2. Materials and methods

2.1. Animals

Animal experiments were approved by the Ethic Committee of Harbin Medical University (Harbin, China). All protocols were complied with the Guide for the Use and Care of Laboratory Animals published by National Institutes of Health (NIH Publication No. 85-23, revised 1996).

Sixty male Kunming mice (20−25 g) were purchased from the Animal Center of the Second Affiliated Hospital of Harbin Medical University (Harbin, China). The animals were subjected to a 12 h dark/light cycle with a constant humidity of 55 ± 5%.

2.2. Mouse model of TAC and emodin administration

Mice were fed for one-week acclimatization. They were then randomly divided into control, transaortic constriction (TAC), TAC+emodin (10, 20, and 40 mg/kg/day, 0.1 mL/10 g) and TAC+captopril (10 mg/kg/day, 0.1 mL/10 g) groups (10 mice in each group). Captopril (Xudong Haipu Pharmaceutical Co., Ltd., Shanghai, China) and emodin (≥98% in purity, Chengdu Pufei De Biotech Co., Ld., Chengdu, China) were dissolved in distilled water before use. The dosages of emodin and captopril were determined according to previous studies[19−21]. Animals were anaesthetized with sodium pentobarbital (6 mg/kg, i.p., Sigma, St. Louis, MO, USA) and the effective anesthesia was verified by a loss of interdigital reflex. Next, TAC was performed as previously described[18]. Emodin or captopril was intragastrically administered into animals daily for four consecutive weeks. Control animals were given an equal volume of saline.

2.3. Cardiac echocardiography

Four weeks after drug administration, mice were anaesthetized with sodium pentobarbital for cardiac echocardiography using an ultrasound machine (Vivid 7, GE Medical System, Milwaukee, WI, USA). The diastolic and systolic left ventricular posterior wall thickness (LVPWd, LVPWs) determined from the M-mode recording was used to evaluate left ventricle thickening[22].

2.4. Masson staining assay

Collagen deposition was detected by Masson trichrome staining as described in our previous study[18]. Briefly, hearts were excised and fixed in 4% paraform, and then embedded in paraffin. The preparations were cut to 5 μm-thick sections. Masson's trichrome staining (Solarbio, Beijing, China) was performed following the manufacturer's introduction. Images were analyzed with Image Pro Plus software (Media Cybernetics, Bethesda, MD, USA) to quantify fibrotic area.

2.5. Cell cultures and transfection

Cardiac fibroblasts and cardiomyocytes were isolated from hearts of neonatal mice (1−3 days old) and cultured as described previously[18]. Fresh Dulbecco's modified Eagle's medium (DMEM, Hyclone, Logan, Utah, USA) containing 10% fetal bovine serum (FBS, Gibco, Grand Island, NY, USA) was added into the culture flask. Cardiac fibroblasts of the second or third passages were used in our experiments.

Adult mice cardiac fibroblasts were isolated as previously described[23,24]. Briefly, mouse heart was removed from anesthetized Kunming mice. The ventricles were dissected, minced, and then digested in collagenase (Gibco) for 30 min, six repeated periods of trypsin (Sigma) at 37 °C for 10 min, followed by another 10 min incubation with collagenase. Then cells

were pelleted by centrifugation (1000 rpm, SC-3610, ZONKIA, Hefei, Anhui, China) for 5 min and re-suspended in DMEM medium.

Mouse aortic endothelial cells (MAECs) were purchased from Beijing Beina Chuanglian Biotechnology Institute (Beijing, China). The cells were cultured in high-glucose DMEM.

Cardiac fibroblasts were transfected with *Mta3* small interfering RNAs (siRNA) or scrambled negative control (NC) siRNA (RiboBio Co., Ltd., Guangzhou, Guangdong, China). The transfection mixture (100 nmol/L) was dissolved in Opti-MEM serum-free medium and added to the cells. *Mta3*-overexpressing pcDNA3.1-plasmid (Invitrogen, Carlsbad, CA, USA) was transfected into cardiac fibroblasts using Lipofectamine 2000 reagent (Invitrogen) according to the manufacturer's instructions. After 6 h of transfection, the medium was replaced by fresh medium containing AngII for 24 h and then treated with or without emodin for 24 h. After drug treatment, the cells were used for protein/RNA extraction.

2.6. Determination of cell number

Cell counting kit 8 (CCK8, Solarbio) and Trypan blue staining assay (Solarbio) were used to measure the number of living fibroblasts as previously described[25,26]. Briefly, 10 μL of CCK8 solution was added onto a 96-well plate seeded with cardiac fibroblasts and incubated for 4 h. Absorbance at 450 nm was recorded.

In trypan blue staining, cells were resuspended and mixed with 0.1% trypan blue at room temperature for 5 min. Cell suspension was counted on an automated cell counter (Countless II FL, Invitrogen) and analyzed for the ratio of living cells[26].

2.7. Transwell migration assay

Cardiac fibroblasts were loaded onto polycarbonated membrane (8 μm pore size, Corning, New York, NY, USA) with DMEM, together with different concentrations of emodin or captopril. DMEM+10% FBS was loaded to the lower side of the migration chamber. After 24 h incubation, non-migrated cells remaining on the upper surface of the membrane were removed with a cotton swab and migrated cells were stained with 0.1% crystal violet for 30 min. Migrated cells were visualized and counted under a microscope (Nikon, Melvill, NY, USA) at 200 × magnification. Five to six fields were counted on each membrane. Triplicate determinations were performed for each experimental condition. Migration is expressed as the mean value of total number of migrated cells per field.

2.8. Real-time PCR

Total RNA was harvested from cells using TRIzol reagent (Invitrogen) according to the manufacturer's protocols[27,28]. cDNA synthesis was performed using a High Capacity cDNA Reverse Transcription Kit (Applied Biosystems, Carlsbad, CA, USA) according to the manufacturer's instructions. The levels of mRNAs were determined by SYBR green I incorporation method and real-time PCR system (ABI7500, Applied Biosystems, Carlsbad, CA, USA). Primer pairs were designed by RiboBio Co., Ltd. *Gapdh* was used as an internal control. Relative mRNA levels were calculated by $2^{-\Delta\Delta Ct}$.

2.9. Western blot

Western blot analysis was performed as previously described[29]. Protein samples were extracted with RIPA buffer (Solarbio) supplemented with protease inhibitors (Sigma) and quantified using the BCA method (Beyotime). Protein samples were fractionated by sodium dodecyl sulfate-polyacrylamide gel electrophoresis (SDS-PAGE, 10% polyacrylamide gels) and transferred to nitrocellulose membrane. After blocking with 5% non-fat milk, the membranes were incubated with the primary antibodies for MTA3 (Absin Bioscience Inc., Shanghai, China), α-smooth muscle actin (α-SMA, Sigma), COL1A2 (Sigma), and GAPDH (Zhongshan Golden Bridge Biotechnology, Beijing, China), followed by incubation with a fluorescence-labeled secondary antibody. The blotted proteins were detected and quantified by Odyssey Infrared Imaging System (LI-COR, Lincoln, NB, USA). GAPDH was used as internal control.

2.10. Immunofluorescent staining

Immunofluorescent staining was performed as previously described[29]. In brief, cardiac fibroblasts were fixed, permeabilized (except for the experiments depicted in Fig. 2C), blocked, and then incubated with primary antibodies at 4 °C overnight. Next, the cells were probed with fluorescence-labeled secondary antibody and DAPI for staining nuclei, and examined under a confocal laser scanning microscope (FV300, Olympus, Tokyo, Japan).

2.11. Statistical analysis

Data are presented as mean ± SEM (standard error of mean). Statistical comparisons were performed with Student's *t*-test between two groups or one-way ANOVA for multiple-group comparisons. $P < 0.05$ was considered to indicate a significant difference. Data were analyzed using the GraphPad Prism 5.0 software.

3. Results

3.1. Emodin reduces cardiac fibrosis in hypertrophic hearts of TAC mice

Oral administration of emodin or positive drug, captopril, for 4 weeks substantially reduced LVPWd, LVPWs, and heart weight/body weight ratio (HW/BW), as well as heart weight/tibia length ratio (HW/TL) in TAC mice (Fig. 1A–C, and Supporting Information Fig. S1). Excess collagen deposition was observed in TAC hearts and this adverse alteration was essentially prevented by emodin treatment (Fig. 1D and E). The effects of emodin were concentration-dependent. Based on these results, we used dosage of 40 mg/kg for our subsequent *in vivo* studies. Consistently, the marker proteins of cardiac fibroblast activation α-SMA and collagen I constitutive protein (COL1A2) were both significantly increased after TAC and these changes were mitigated by emodin (Fig. 2A–D).

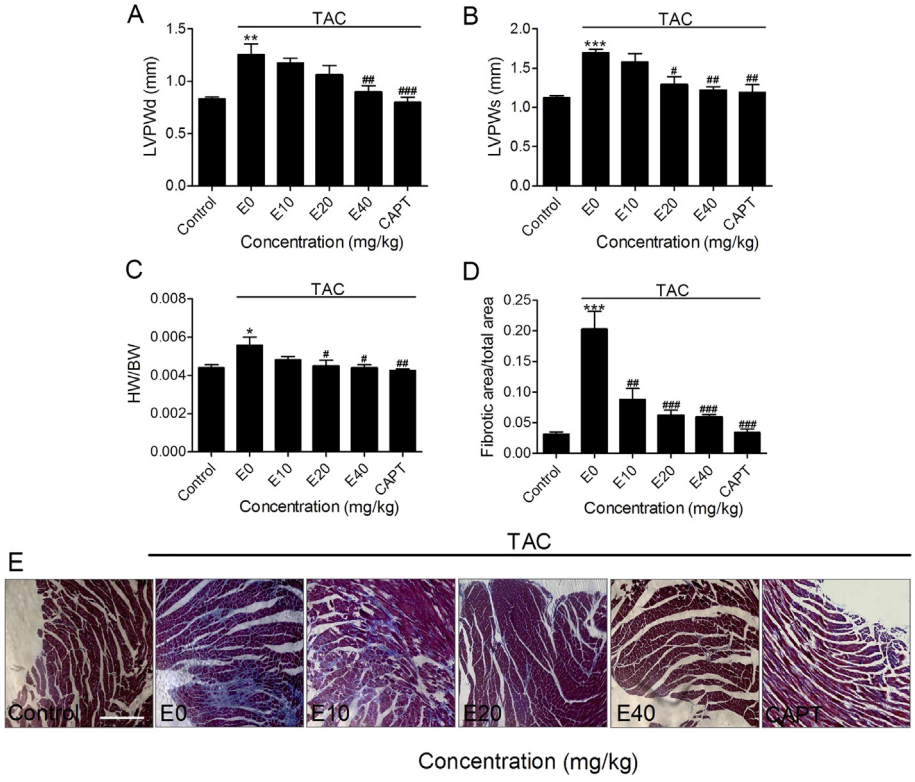

Figure 1 Emodin reduces the thickened left ventricle in pressure overload mice. (A)−(C) Effects of varying dosages of emodin (10, 20, and 40 mg/kg/day) and captopril (10 mg/kg) on diastolic and systolic left ventricular posterior wall (LVPWd, LVPWs) thickness, heart weight/body weight (HW/BW) in transaortic constriction (TAC) mice ($n = 5$ batches in each group). E0 represents the non-emodin treated group; E10, E20, and E40 represent mice treated with 10, 20, and 40 mg/kg emodin, respectively. CAPT represents the 10 mg/kg captopril group. $^{*}P < 0.05$, $^{**}P < 0.01$, $^{***}P < 0.001$ compared with control group; $^{\#}P < 0.05$, $^{\#\#}P < 0.01$, $^{\#\#\#}P < 0.001$ compared with TAC+E0 group. (D) Statistic data of fibrotic area/total area and (E) representative images of Masson trichrome-stained sections showing the collagen deposition and relief of such adverse alteration by emodin ($n = 3$). $^{***}P < 0.001$ compared with control group; $^{\#\#}P < 0.01$, $^{\#\#\#}P < 0.001$ compared with TAC+E0 group. Scale bar = 50 μm.

3.2. *Emodin inhibits activation of cardiac fibroblasts stimulated by AngII*

Excess activation of cardiac fibroblasts, including increased proliferation, migration and collagen synthesis, is a key step for cardiac fibrosis, and suppression of such a process is expected to reduce fibrosis[30]. As shown in Fig. 3, emodin significantly decreased the ability of migration, number of living cardiac myofibroblasts in the presence of AngII; in other words, compared with controls and captopril group, emodin reversed the AngII-induced increase in cardiac myofibroblasts. The inhibitory effect of emodin was concentration-dependent with around 50% reduction at a concentration of 20 μmol/L. Thus, this emodin concentration (20 μmol/L) was employed in our subsequent *in vitro* experiments.

As expected, emodin significantly mitigated the upregulation of α-SMA and synthesis of collagen I induced by AngII (Fig. 4).

3.3. *MTA3 as an anti-fibrotic regulator mediating the beneficial action of emodin*

Our previous study has demonstrated that silence of MTA3 expression contributes to the development of cardiac fibrosis[18]. Here, we wanted to test whether MTA3 is involved in the beneficial action of emodin on cardiac fibrogenesis. As shown in Fig. 5A, MTA3 was found abundantly expressed in cardiac fibroblasts with minimal expression in cardiac myocytes and endothelial cells. MTA3 was significant reduced in TAC hearts and in AngII-stimulated cardiac fibroblasts as well, and emodin restored this downregulation back to normal level by 0.92 ± 0.08-fold as in control hearts without TAC and 1.00 ± 0.11-fold *versus* cardiac fibroblasts without AngII treatment (Fig. 5B−E).

To clarify if upregulation of MTA3 mediates the anti-fibrotic action of emodin, we artificially silenced MTA3 expression using a siRNA for *Mta3* gene (siMTA3) and then looked at the changes of fibrotic phenotypes. As depicted in Fig. 6 and Supporting Information Fig. S2, efficient silence of MTA3 expression (Fig. 6A) mitigated the beneficial effects of emodin on cardiac fibrosis. Specifically, siMTA3 abrogated the downregulation of fibrotic markers α-SMA and COL1A2 (Fig. 6B and C), decreases in cell viability and number (Fig. 6D and E). The negative control construct of siMTA3 failed to affect the fibrotic phenotypes.

As anticipated, silence of MTA3 expression alone in cardiac fibroblasts under normal conditions without treatment with AngII and emodin markedly upregulated the protein and mRNA levels of α-SMA and COL1A2 (Fig. 7 and Supporting Information Fig. S3).

While the above results suggest MTA3 as an anti-fibrotic factor, the following experiments with a gain-of-function

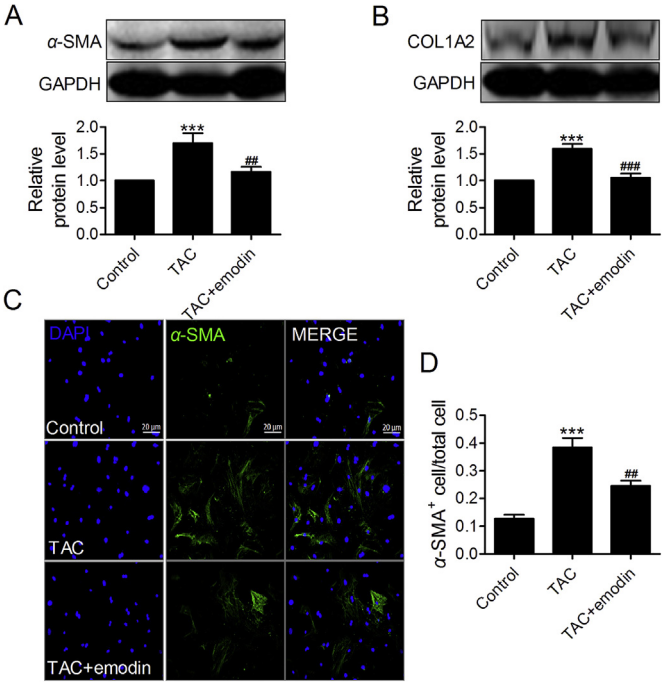

Figure 2 Emodin represses the activation of cardiac fibroblasts in pressure overload mice. (A) and (B) α-SMA and COL1A2 protein levels detected by Western blotting showing the inhibitory effects of emodin (40 mg/kg/day) on the expression of these biomarkers for fibroblast activation in heart tissues, normalized to GAPDH. The data are presented as relative levels (A, $n = 14$; B, $n = 7$). $^{***}P < 0.001$ compared with control group; $^{\#\#}P < 0.01$, $^{\#\#\#}P < 0.001$ compared with TAC group. (C) Determination of α-SMA-positive cells by immunofluorescent staining in cardiac fibroblasts isolated from adult mice. (D) Statistical data on the number of α-SMA positive cells ($n = 5$ batches in each group). $^{***}P < 0.001$ compared with control group; $^{\#\#}P < 0.01$ compared with TAC group. Scale bar = 20 μm.

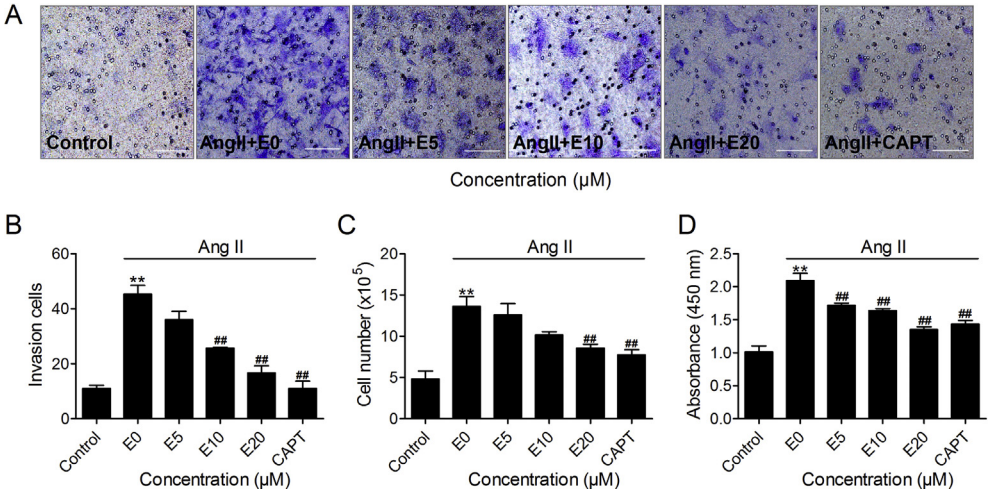

Figure 3 Emodin suppresses viability and migration of cardiac fibroblasts stimulated by angiotensin II (AngII). (A) and (B) Results of transwell analysis depicting the effects of emodin on the migration ability of cardiac fibroblasts stimulated by AngII. E0 represents non-emodin cardiac fibroblasts; E5, E10, and E20 represent 5, 10, and 20 μmol/L emodin, respectively. CAPT represents 10 μmol/L captopril treated group ($n = 3$ batches in each group). $^{***}P < 0.001$ compared with control group; $^{\#\#\#}P < 0.001$ compared with AngII+E0 group. (C) Effects of emodin on cell number measured by trypan blue staining analysis ($n = 7$). $^{***}P < 0.001$ compared with control group; $^{\#\#}P < 0.01$, $^{\#\#\#}P < 0.001$ compared with AngII+E0 group. (D) Effects of emodin on the number of living fibroblasts detected by cell counting kit 8 (CCK8) assay ($n = 5$). $^{***}P < 0.001$ compared with control group; $^{\#\#}P < 0.01$, $^{\#\#\#}P < 0.001$ compared with AngII+E0 group. Scale bar = 20 μm.

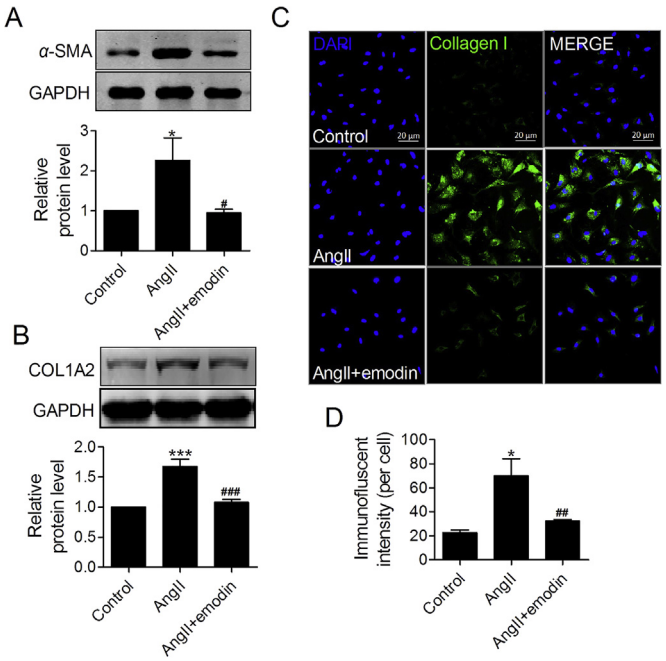

Figure 4 Emodin downregulates α-smooth muscle actin (α-SMA) and COL1A2 in AngII-stimulated cardiac fibroblasts. (A) and (B) α-SMA and COL1A2 protein levels detected by Western blot in cardiac fibroblasts, normalized to GAPDH. Data are presented as relative levels ($n = 5$). $^{*}P < 0.05$, $^{***}P < 0.001$ compared with control group; $^{\#}P < 0.05$, $^{\#\#\#}P < 0.001$ compared with AngII group. (C) and (D) Immunofluorescent staining of collagen I and the statistical data ($n = 5$ in each group). $^{*}P < 0.05$ compared with control group; $^{\#\#}P < 0.01$ compared with AngII group.

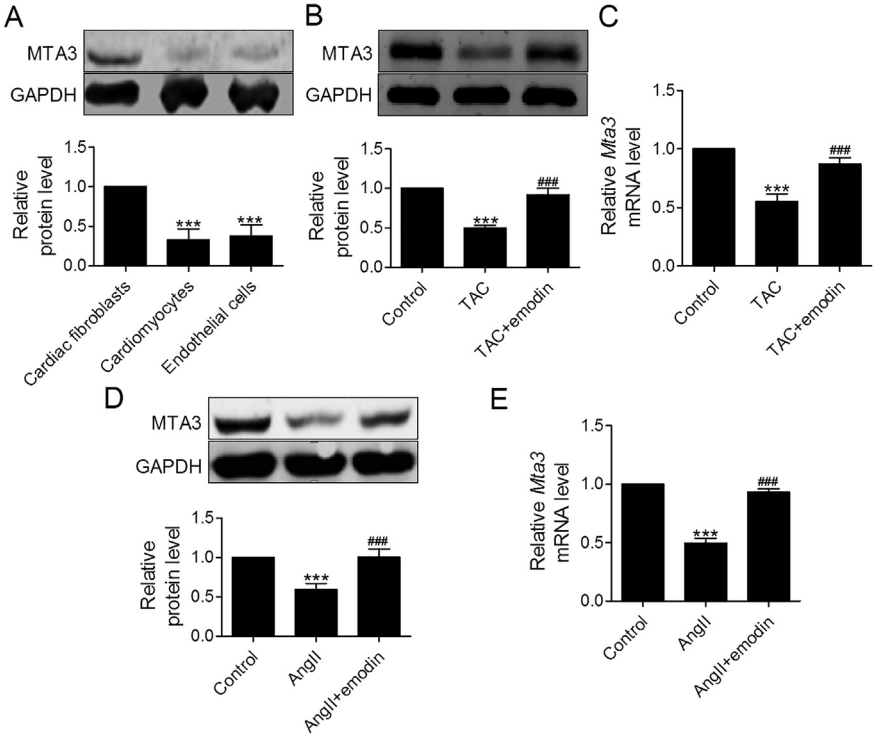

Figure 5 Emodin upregulates metastasis associated protein 3 (MTA3) expression. (A) Comparison of MTA3 abundance in cardiac fibroblasts, cardiomyocytes, and endothelial cells, as determined by Western blot. Averaged data were normalized to GAPDH ($n = 3$). $^{***}P < 0.001$. (B) and (C) Effects of emodin on MTA3 expression at both protein and mRNA levels in TAC mice, as determined by Western blot (B, $n = 11$) and real-time PCR (C, $n = 5$), respectively. $^{***}P < 0.001$ compared with control group; $^{\#\#\#}P < 0.001$ compared with TAC group. (D) and (E) Effects of emodin on MTA3 expression at both protein and mRNA levels in cardiac fibroblasts pretreated with AngII, as determined by Western blot (D, $n = 5$) and real-time PCR (E, $n = 3$), respectively. $^{***}P < 0.001$ compared with control group; $^{\#\#\#}P < 0.001$ compared with TAC group.

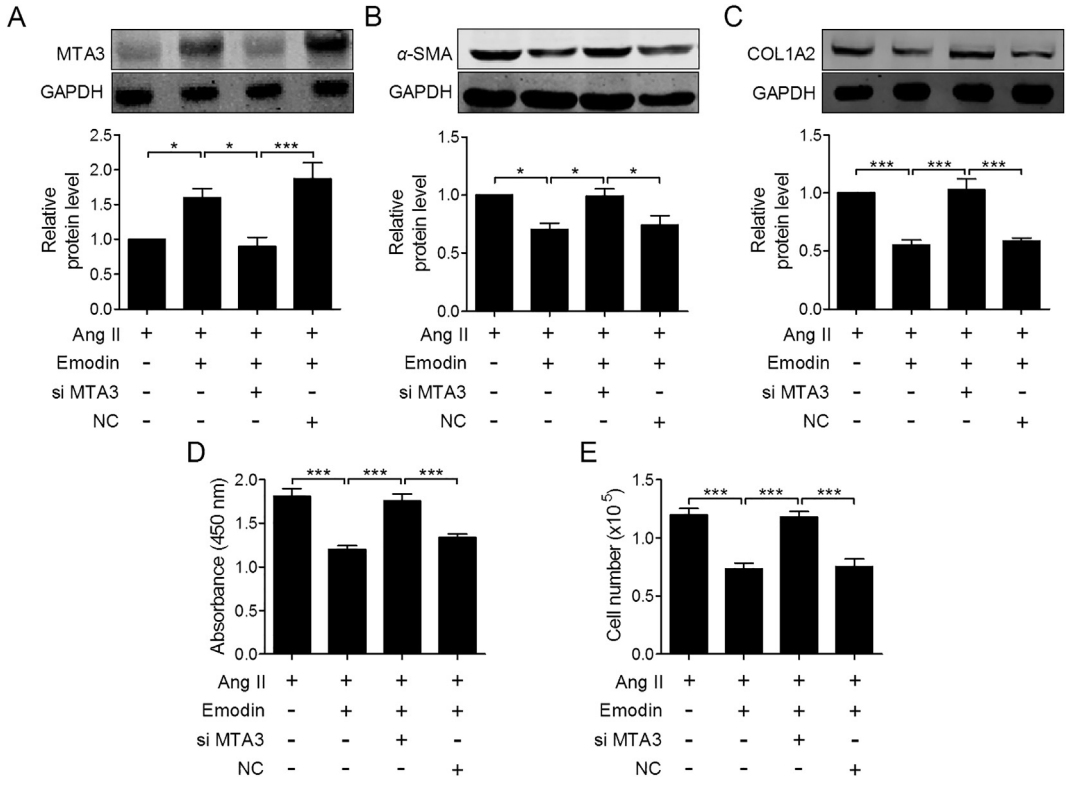

Figure 6 Silence of MTA3 blocks the inhibitory effect of emodin on cardiac fibroblasts overproliferation. Cardiac fibroblasts were transfected with *Mta3* small interfering RNA (siMTA3) or negative control (NC) in the presence of AngII with or without emodin. (A)−(C) Effects of siMTA3 on the protein levels of MTA3, α-SMA and COL1A2 ($n = 5$). $^{*}P < 0.05$, $^{***}P < 0.001$. (D) Effects of siMTA3 on the number of living cells as detected by CCK8 assay ($n = 5$). $^{***}P < 0.001$. (E) Effects of siMTA3 on cell number as measured by Trypan blue staining ($n = 5$). $^{***}P < 0.001$.

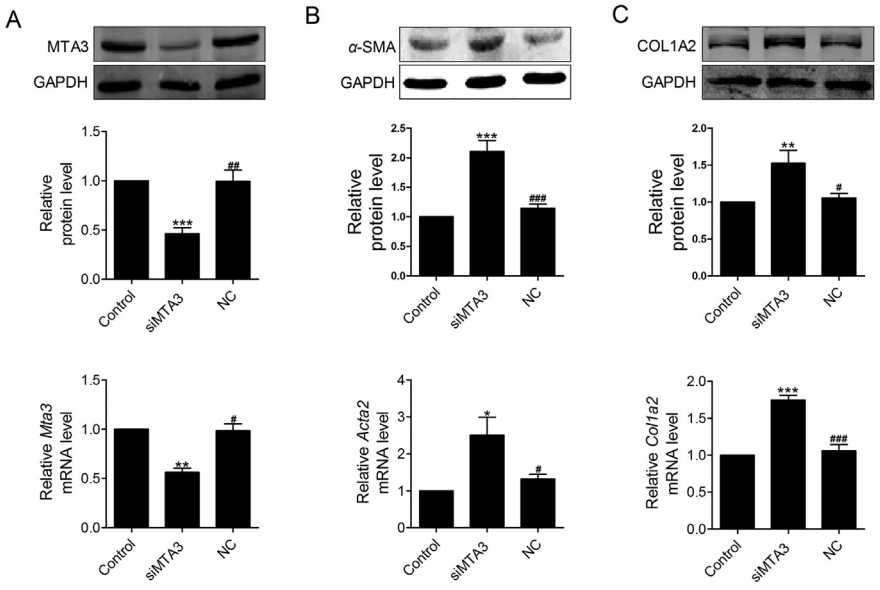

Figure 7 Silence of MTA3 expression promotes cardiac fibrosis. Cardiac fibroblasts were transfected with siMTA3 or NC. (A) Verification of the efficacy of MTA3 silence by siMTA3 at both protein (upper panel) and mRNA (lower panel) levels ($n = 5$). $^{**}P < 0.01$ compared with control group; $^{\#}P < 0.05$, $^{\#\#}P < 0.01$ compared with NC group. (B) and (C) Effects of siMTA3 on the expression of α-SMA and COL1A2 at both protein (upper panels) and mRNA (lower panels) levels ($n = 5$; except for mRNA in C, $n = 4$). $^{*}P < 0.05$, $^{**}P < 0.01$, $^{***}P < 0.001$ compared with control group; $^{\#}P < 0.05$, $^{\#\#}P < 0.01$, $^{\#\#\#}P < 0.001$ compared with NC group.

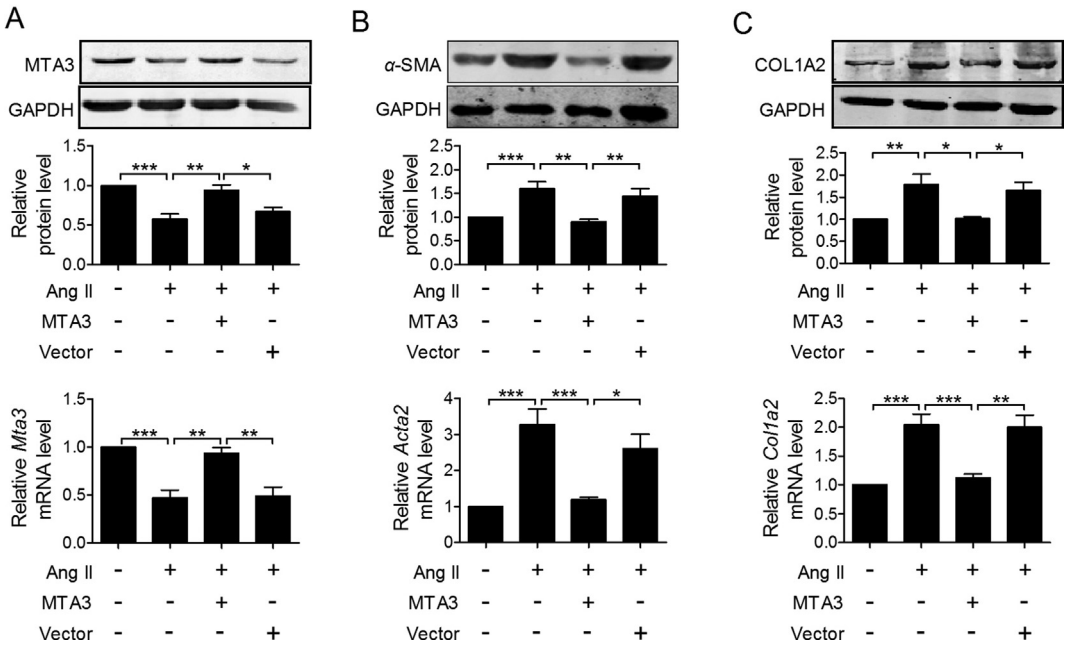

Figure 8 Overexpression of MTA3 in regulating cardiac fibrosis. (A) Verification of MTA3 overexpression at both protein (upper panel) and mRNA (lower panel) levels ($n = 5$). $^{*}P < 0.05$, $^{**}P < 0.01$, $^{***}P < 0.001$. (B) and (C) Effects of MTA3 overexpression on protein (upper panels) and mRNA (lower panels) levels of α-SMA and COL1A2 in cardiac fibroblasts stimulated by AngII ($n = 5$ for protein; $n = 5$ for mRNA). $^{*}P < 0.05$, $^{**}P < 0.01$, $^{***}P < 0.001$.

approach further supported the notion. Transfection of the plasmid vector for MTA3 overexpression (Fig. 8A) into cardiac fibroblasts produced beneficial effects as emodin did. As illustrated in Fig. 8B and C, MTA3 overexpression suppressed the AngII-induced upregulation of hypertrophic marker α-SMA (Fig. 8B) and COL1A2 (Fig. 8C). The empty vector for control affected neither MTA3 levels nor the expression of α-SMA and COL1A2.

4. Discussion

Cardiac fibrosis has been recognized as a causal factor leading to the eventual development of heart failure[31]. It has been identified as a long-standing condition caused by various pathogenic stimuli, such as hypertension-induced pressure overload[32]. This study set out with the aim of assessing the beneficial effects and underlying mechanisms of emodin on cardiac fibrosis. We first observed that emodin alleviated TAC-induced cardiac fibrosis and AngII-stimulated activation of cardiac fibroblasts. Then, in agreement with the results of our previous study[18], we found that the emodin/MTA3 axis played a crucial role in regulating cardiac fibrosis. Finally, with both loss- and gain-of-function approaches, we identified MTA3 as an important regulator of activation of cardiac fibroblasts.

Interactions between emodin and several pathological conditions have recently been reviewed in detail[4]. Xu et al[33]. demonstrated that emodin inhibited TNFα-induced calcification of human aortic valve interstitial cells. Zeng et al[34]. revealed emodin as a novel candidate agent for hyperhomocysteinemia-induced dementia and Alzheimer's disease-like symptoms. Hwang et al[35]. reported that emodin exerted anti-inflammatory effects in collagen-induced arthritic mice through inhibition of the NF-κB pathway and therefore may have therapeutic value for the treatment of rheumatoid arthritis. Recent studies have identified the anti-tumor property of emodin with high selectivity towards diseased lesions. Zu et al[36]. reported that low-dose emodin induced tumor senescence for boosting breast cancer chemotherapy *via* silencing NRARP. In spite of a long history of emodin applications since first reported in 1925[9], little is known about its pharmacological properties until recent decades. Guan et al[37]. reported that emodin ameliorated bleomycin-induced pulmonary fibrosis suppressing epithelial−mesenchymal transition and fibroblast activation. Wang et al[11]. showed that emodin reduced the peritoneal fibrosis related to dialysis. However, it remained unstudied whether emodin can also regulate cardiac fibrosis, one of the most severe chronic diseases in the world.

The role of MTA3 in regulating multiple cellular events has been recognized[38]. As a transcriptional factor, MTA3 is believed to indirectly modulate the progression of epithelium−mesenchymal transition, and subsequently represses the proliferation, invasion and migration of cancer cells by acting on snail[14]. MTA3 also accelerates the differentiation of breast cancer cells[39]. Apparently, in addition to act a tumor suppressor, MTA3 also has other cellular and pathophysiological roles. Our previous study revealed that MTA3 mediated the anti-fibrotic effect of genistein in the heart[18]. Here, we further demonstrated upregulation of MTA3 as a molecular mechanism by which emodin suppressed cardiac fibrosis in the setting of cardiac hypertrophy.

It is not known at present how exactly emodin upregulates expression of MTA3. The fact that emodin increased MTA3 expression at both mRNA and protein levels with a similar degree of changes would suggest a regulatory role in the transcriptional level. Yet this note needs rigorous studies to clarify. Nonetheless, it is likely that as a pharmacologic agent, emodin acts primarily through indirect mechanism(s) to modulate activation and/or level of some relevant transcription factors that in turn alter MTA3 transcription.

5. Conclusions

The results demonstrate that emodin alleviates cardiac fibrosis through inhibiting the activation of cardiac fibroblasts by regulating MTA3. The findings strengthen the idea that traditional Chinese medication might be a novel agent to improve the clinical treatment of cardiac fibrosis.

Acknowledgments

This work was supported in part by the National Key R&D Program of China (2017YFC1702003), the National Natural Science Foundation of China (81570399/81773735/81811530117), and Heilongjiang Outstanding Youth Science Fund (JJ2017JQ0035, China).

Appendix A. Supporting information

Supporting data to this article can be found online at https://doi.org/10.1016/j.apsb.2019.04.003.

References

1. Zhou Y, Deng L, Zhao D, Chen L, Yao Z, Guo X, et al. Microrna-503 promotes angiotensin II-induced cardiac fibrosis by targeting apelin-13. *J Cell Mol Med* 2016;**20**:495−505.
2. Kong P, Christia P, Frangogiannis NG. The pathogenesis of cardiac fibrosis. *Cell Mol Life Sci* 2014;**71**:549−74.
3. Tao H, Yang JJ, Shi KH, Li J. Wnt signaling pathway in cardiac fibrosis: new insights and directions. *Metabolism* 2016;**65**:30−40.
4. Dong X, Fu J, Yin X, Cao S, Li X, Lin L, et al. Emodin: a review of its pharmacology, toxicity and pharmacokinetics. *Phytother Res* 2016;**30**:1207−18.
5. Hei ZQ, Huang HQ, Tan HM, Liu PQ, Zhao LZ, Chen SR, et al. Emodin inhibits dietary induced atherosclerosis by antioxidation and regulation of the sphingomyelin pathway in rabbits. *Chin Med J (Engl)* 2006;**119**:868−70.
6. Song ZC, Wang ZS, Bai JH, Li Z, Hu J. Emodin, a naturally occurring anthraquinone, ameliorates experimental autoimmune myocarditis in rats. *Tohoku J Exp Med* 2012;**227**:225−30.
7. Nemmar A, Al Dhaheri R, Alamiri J, Al Hefeiti S, Al Saedi H, Beegam S, et al. Diesel exhaust particles induce impairment of vascular and cardiac homeostasis in mice: ameliorative effect of emodin. *Cell Physiol Biochem* 2015;**36**:1517−26.
8. Chen Q, Pang L, Huang S, Lei W, Huang D. Effects of emodin and irbesartan on ventricular fibrosis in goldblatt hypertensive rats. *Pharmazie* 2014;**69**:374−8.
9. Monisha BA, Kumar N, Tiku AB. Emodin and its role in chronic diseases. *Adv Exp Med Biol* 2016;**928**:47−73.
10. Yang T, Wang J, Pang Y, Dang X, Ren H, Liu Y, et al. Emodin suppresses silica-induced lung fibrosis by promoting Sirt1 signaling *via* direct contact. *Mol Med Rep* 2016;**14**:4643−9.
11. Wang HC, Lin XH, Fang XP, Mu XY, Li TJ, Liu JL. Emodin ameliorates the peritoneal dialysis-related peritoneal fibrosis *via* inhibiting the activation of notch pathway. *Sheng Li Xue Bao* 2016;**68**:747−56.
12. Du L, Ning Z, Zhang H, Liu F. Corepressor metastasis-associated protein 3 modulates epithelial-to-mesenchymal transition and metastasis. *Chin J Canc* 2017;**36**:28.
13. Chen Y, Khoo SK, Leach R, Wang K. MTA3 regulates extravillous trophoblast invasion through NuRD complex. *AIMS Med Sci* 2017;**4**:17−27.
14. Ma L, Yao Z, Deng W, Zhang D, Zhang H. The many faces of MTA3 protein in normal development and cancers. *Curr Protein Pept Sci* 2016;**17**:726−34.
15. Deb A, Ubil E. Cardiac fibroblast in development and wound healing. *J Mol Cell Cardiol* 2014;**70**:47−55.
16. Ding D, Zhang Y, Wen L, Fu J, Bai X, Fan Y, et al. Mir-367 regulates cell proliferation and metastasis by targeting metastasis-associated protein 3 (MTA3) in clear-cell renal cell carcinoma. *Oncotargets* 2017;**8**:63084−95.
17. Guo F, Hutchenreuther J, Carter DE, Leask A. TAK1 is required for dermal wound healing and homeostasis. *J Investig Dermatol* 2013;**133**:1646−54.
18. Qin W, Du N, Zhang L, Wu X, Hu Y, Li X, et al. Genistein alleviates pressure overload-induced cardiac dysfunction and interstitial fibrosis in mice. *Br J Pharmacol* 2015;**172**:5559−72.
19. Zhang J, Hu Z, Chen Z. Inhibitory effect of emodin on the growth of cervical cancer in tumor-transplanted mice and underlying mechanism. *J Cell Mol Immunol* 2015;**31**:350−4.
20. Van der Mieren G, Nevelsteen I, Vanderper A, Oosterlinck W, Flameng W, Herijgers P. Angiotensin-converting enzyme inhibition and food restriction restore delayed preconditioning in diabetic mice. *Cardiovasc Diabetol* 2013;**12**:36.
21. Liu JX, Zhang JH, Li HH, Lai FJ, Chen KJ, Chen H, et al. Emodin induces PANC-1 cell apoptosis *via* declining the mitochondrial membrane potential. *Oncol Rep* 2012;**28**:1991−6.
22. Luo T, Chen B, Wang X. 4-PBA prevents pressure overload-induced myocardial hypertrophy and interstitial fibrosis by attenuating endoplasmic reticulum stress. *Chem Biol Interact* 2015;**242**:99−106.
23. Ackers-Johnson M, Li PY, Holmes AP, O'Brien SM, Pavlovic D, Foo RS. A simplified, langendorff-free method for concomitant isolation of viable cardiac myocytes and nonmyocytes from the adult mouse heart. *Circ Res* 2016;**119**:909−20.
24. Li R, Gong K, Zhang Z. Isolation, purification and primary culture of adult mouse cardiac fibroblasts. *J Cell Mol Immunol* 2017;**33**:67−71.
25. Wang H, Yang X, Yang Q, Gong L, Xu H, Wu Z. PARP-1 inhibition attenuates cardiac fibrosis induced by myocardial infarction through regulating autophagy. *Biochem Biophys Res Commun* 2018;**503**:1625−32.
26. Zhang Z, Zhang G, Kong C. Targeted inhibition of POLO-like kinase 1 by a novel small-molecule inhibitor induces mitotic catastrophe and apoptosis in human bladder cancer cells. *J Cell Mol Med* 2017;**21**:758−67.
27. Zhang Y, Li X, Li J, Zhang Q, Chen X, Liu X, et al. The antihyperglycemic efficacy of a lipid-lowering drug daming capsule and the underlying signaling mechanisms in a rat model of diabetes mellitus. *Sci Rep* 2016;**6**:34284.
28. Zhang Y, Li X, Zhang Q, Li J, Ju J, Du N, et al. Berberine hydrochloride prevents postsurgery intestinal adhesion and inflammation in rats. *J Pharmacol Exp Ther* 2014;**349**:417−26.
29. Xiao D, Zhou T, Fu Y, Wang R, Zhang H, Li M, et al. Microrna-17 impairs glucose metabolism in insulin-resistant skeletal muscle *via* repressing glucose transporter 4 expression. *Eur J Pharmacol* 2018;**838**:170−6.
30. Deng P, Chen L, Liu Z, Ye P, Wang S, Wu J, et al. MicroRNA-150 inhibits the activation of cardiac fibroblasts by regulating c-Myb. *Cell Physiol Biochem* 2016;**38**:2103−22.
31. Jin L, Sun S, Ryu Y, Piao ZH, Liu B, Choi SY, et al. Gallic acid improves cardiac dysfunction and fibrosis in pressure overload-induced heart failure. *Sci Rep* 2018;**8**:9302.
32. Matsushita N, Ishida N, Ibi M, Saito M, Sanbe A, Shimojo H, et al. Chronic pressure overload induces cardiac hypertrophy and fibrosis *via* increases in *Sglt1* and *Il-18* gene expression in mice. *Int Heart J* 2018;**59**:1123−33.
33. Xu K, Zhou T, Huang Y, Chi Q, Shi J, Zhu P, et al. Anthraquinone emodin inhibits tumor necrosis factor α-induced calcification of human aortic valve interstitial cells *via* the NF-κB pathway. *Front Pharmacol* 2018;**9**:1328.
34. Zeng P, Shi Y, Wang XM, Lin L, Du YJ, Tang N, et al. Emodin rescued hyperhomocysteinemia-induced dementia and Alzheimer's disease-like features in rats. *Int J Neuropsychopharmacol* 2019;**22**:57−70.

35. Hwang JK, Noh EM, Moon SJ, Kim JM, Kwon KB, Park BH, et al. Emodin suppresses inflammatory responses and joint destruction in collagen-induced arthritic mice. *Rheumatology (Oxford)* 2013;**52**: 1583−91.
36. Zu C, Qin G, Yang C, Liu N, He A, Zhang M, et al. Low dose emodin induces tumor senescence for boosting breast cancer chemotherapy *via* silencing NRARP. *Biochem Biophys Res Commun* 2018;**505**: 973−8.
37. Guan R, Wang X, Zhao X, Song N, Zhu J, Wang J, et al. Emodin ameliorates bleomycin-induced pulmonary fibrosis in rats by suppressing epithelial-mesenchymal transition and fibroblast activation. *Sci Rep* 2016;**6**:35696.
38. Jiao T, Li Y, Gao T, Zhang Y, Feng M, Liu M, et al. MTA3 regulates malignant progression of colorectal cancer through Wnt signaling pathway. *Tumour Biol* 2017;**39**. 1010428317695027.
39. Dong H, Guo H, Xie L, Wang G, Zhong X, Khoury T, et al. The metastasis-associated gene *MTA3*, a component of the Mi-2/NuRD transcriptional repression complex, predicts prognosis of gastroesophageal junction adenocarcinoma. *PLoS One* 2013;**8**: e62986.